Journal of Achievements in Materials and Manufacturing Engineering
International Scientific Journal published monthly by the World Academy of Materials and Manufacturing Engineering

Background of branched crack formation in surface zone of continuously-cast Ti-Nb microalloyed steel slab

P. Bekeč [a,b,*], M. Longauerová [b], M. Vojtko [b], O. Milkovič [b], J. Kadlec [c], G. Tréfa [d], G. Grimplini [d]

[a] ŽP Research and Development Centre, Kolkáreň 35, 976 81 Podbrezová, Slovakia
[b] Department of Materials Science, Technical University of Košice, Park Komenského 11, 042 00 Košice, Slovakia
[c] SVÚM a.s., Institute of Research Area, Podnikatelská 565, 190 11 Praha 9 - Běchovice, Czech Republic
[d] U.S.STEEL Košice, s.r.o., Research and Development Centre, 044 54 Košice, Slovakia
* Corresponding e-mail address: bekec@zelpo.sk

Received 28.09.2014; published in revised form 01.12.2014

ABSTRACT

Purpose: This work deals with the study of the background to the formation of branched cracks in a continuously-cast slab, at pulling rate 0.43 m.min^{-1}.

Design/methodology/approach: Samples were taken from the individual cut-outs for further analyzes. Macroscopic analysis was used to evaluate the surface quality of the analysed slabs using a Leica Wild M3Z macroscope. The microstructure was observed with an OLYMPUS VANOX-T light microscope. For the evaluation of the concentration profile of the selected elements in planes parallel to the slab surface, wavelength dispersive X-ray analysis (WDX) was used with a Camebax-MICROanalyzer.

Findings: The results of the work show that branched cracks extended to a depth of 10 mm below the slab surface and occurred mostly below oscillation marks. Cracks were mostly present in the edge parts of the slab, where they were also deeper in comparison with locations in the middle of the slab width. Microstructural analysis confirmed heterogeneity of ferrite grain sizes in the slab surface skin. Wavelength-dispersive X-ray analysis of a sample with a branched crack showed chemical heterogeneity of harmful elements, mainly S and As.

Research limitations/implications: Precipitation of microalloying elements in connection with the cementite can lead to higher probability of surface crack formation, as also confirmed in this study.

Originality/value: of this work is background of branched crack formation in surface zone of continuously-cast Ti-Nb microalloyed steel slab.

Keywords: Slab; Branched cracks; Oscillation marks; Segregation; Precipitation

Reference to this paper should be given in the following way:

P. Bekeč, M. Longauerová, M. Vojtko, O. Milkovič, J. Kadlec, G. Tréfa, G. Grimplini, Background of branched crack formation in surface zone of continuously-cast Ti-Nb microalloyed steel slab, Journal of Achievements in Materials and Manufacturing Engineering 67/2 (2014) 58-64.

PROPERTIES

1. Introduction

Branched cracks are also known as net, star or spider cracks. These cracks have branched, irregular shape. They can be present individually, in groups or create networks. They may extend to a depth of 10 mm below the slab surface [1]. The main cause of crack formation is high-temperature plasticity decrease by weakening of phase interfaces. This weakening may be due to [1,2]: segregation of impurities (Sn, As, Sb, S, P), brittle cementite network or low-melting phases. High-strength steels with a low M/S ratio on the occurrence of branched cracks are susceptible, because they may produce sulfides (Fe,Mn),S with a high proportion of Fe as precipitates or inclusions may be excluded on the γ-grains boundaries. These precipitates have a great influence on the initiation of intercrystalline cracks [1]. In their work [3], Marek and Ševčík described the most common defects on the continuously-cast slab surface, and they divided them into groups of visually identifiable defects (e.g. longitudinal and transverse cracks), and included a group of practically undetectable visual defects (e.g., networks of hairline cracks, endogenous inclusions, subsurface bubbles). According to these researchers the most dangerous are fine hairline cracks which spread along the weakened γ-grain boundaries, and this weakening occurs when the slab surface undergoes local carburizing or occupation by small particles (oxidation products) [3]. According to the authors of works [4,5], carburization of the slab surface occurs due to the use of casting powder with a higher content of free carbon. Carbon diffuses at high temperatures from carburized sites into subsurface areas along the boundaries of γ-grains. At the grain boundaries below the transition temperature a brittle cementite network is formed that cracks due to tensile stress when slabs are straightened, whereby branched cracks are formed [4,5]. The aim of this work was to study the background of branched crack formation in a continuously-cast slab made from Ti-Nb microalloyed steel in terms of structural, chemical and phase analysis.

2. Material and experimental methods

A transition slab of Ti-Nb microalloyed steel cast with initial pulling rate 0.43 $m \cdot min^{-1}$ and final rate 0.9 $m \cdot min^{-1}$ was analyzed. Table 1 shows the chemical composition of the analysed slab. Cut-outs were taken from the slab towards its slower cast end, i.e. 0.43 $m \cdot min^{-1}$ as shown in Fig. 1. Samples were taken from the individual cut-outs for further analyzes. Macroscopic analysis was used to evaluate the surface quality of the analysed slabs using a Leica Wild M3Z macroscope. The microstructure was observed with an OLYMPUS VANOX-T light microscope. Each sample was wet ground and polished on DP-Mol polishing discs with 3 μm diamond paste and further polished on MicroCloth discs using the OP-S Suspension system. For etching 2% Nital was applied. Fractures obtained after the crack opening were analyzed with a Jeol - 7000 F scanning electron microscope (SEM) and particles were examined using EDS analysis with an INCAx-sight analyzer.

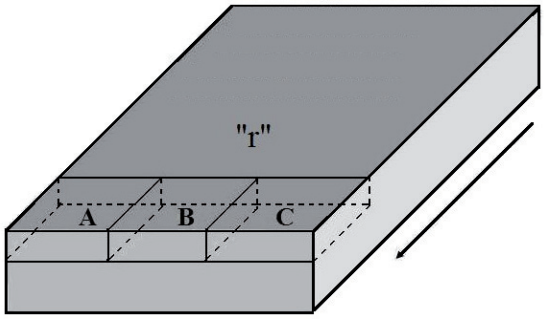

Fig. 1. The cut-out positions and pulling direction of the slab

For the evaluation of the concentration profile of the selected elements in planes parallel to the slab surface, wavelength dispersive X-ray analysis (WDX) was used with a Camebax-MICRO analyzer. Sample A36 was used for measurement with dimensions 20x20x10 mm carved from the surface zone of marginal cut-out A. The metallographic sample was prepared in cross section with respect to the slab pulling direction. The sample was characterized by the presence of branched cracks of depth 5.5 mm below the oscillation marks (OM), where concentration measurements of elements were carried out. Fig. 2 shows a scheme indicating the measurement locations 4 to 7 which represent the measurement plane at depths of 1, 4, 8 and 12 mm below the OM. The final method used was diffraction of hard X-ray radiation, carried out at the experimental station on PO2.1 localized on the PETRA III positron accelerator at HASYLAB / DESY in Hamburg. Sample C12 with OM of dimensions 10x10x5 mm from the surface area from marginal cut-out C was used for analysis, whereby after grinding the slab surface cracks were localized below the OM. By grinding to a depth of 2 mm from the slab surface and the underside of the samples as well, the final thickness of the sample after grinding intended for diffraction analysis reached ~ 1 mm. Hence diffraction analysis was performed in effect at a depth of ~ 2 mm below the slab surface.

Table 1.
Chemical composition of the analysed slab (wt.%)

C	Mn	Si	P	S	Al	Mo	Ti	V
0.082	0.899	0.011	0.011	0.007	0.033	0.002	0.012	0.001
Nb	N_2	Cu	Ni	As	Sn	Zr	Cr	B
0.035	0.0061	0.032	0.014	0.004	0.009	0.001	0.014	0.0002

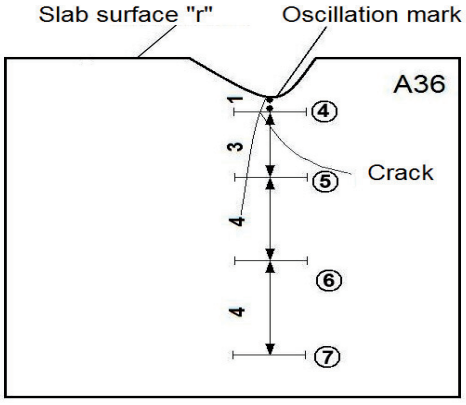

Fig. 2. Scheme of locations for measuring concentration profiles in sample A36

The beam of photons was directed so as to pass through the area of the crack. Samples were irradiated for a period of 20 seconds by photon beam with energy of 58 keV (λ = 20.7271 pm) with an effective cross section of 0.5x0.5 mm^2. The diffractive image was recorded with a Perkin Elmer 1621 2D detector and subsequently integrated into the dependence of intensity-angle (2Θ) using FIT2D software. The distance of the detector from the sample, orthogonal deposition of the detector towards the sheaf, determination of the center of the detector, as well as calculation of the energy of radiation, were all effected by measuring the reference sample CeO_2.

3. Results

Macroscopic analysis of the surface cut-outs showed that no superficial cracks were visible on the surface. Only OM of various depths are visible. The average depth of marks was 0.7 mm, and max. depth reached 2.5 mm. After removal of the test samples from cut-outs A, B and C, cracks were found mostly below the OM. After grinding and polishing of the surface they were found to be branched cracks, and these cracks in some cases extended to a depth of 10 mm below the slab surface. More cracks were found in the marginal cut-outs A and C in comparison with central cut-out B, and they ranged deeper below the slab surface. Microstructural analysis showed heterogeneity in the ferrite grain size in the surface skin, as demonstrated in work [6]. The microstructure was mostly polyhedral ferritic-pearlitic. It was further demonstrated that tertiary cementite was present on the ferritic grain boundaries. The presence of cementite was confirmed by EDX analysis. It was present either in the form of small oval particles or in form of a network. In the marginal cut-outs in addition to polyhedral microstructure, non-equilibrium microstructure of acicular character was also observed, often in the area around the cracks (Fig. 3).

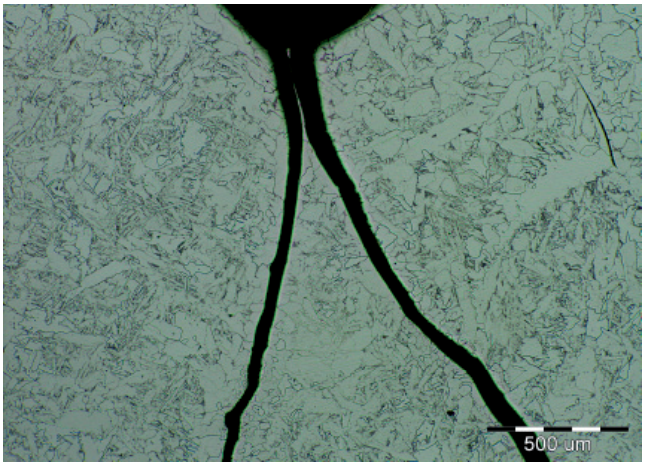

Fig. 3. Detail of branched crack below the OM

Fracture surfaces obtained by crack opening on samples taken from the surface skin were characterized by the presence of coarse intercrystalline facets (Fig. 4) in the surface skin, which ranged in depth to max. 7 mm below the slab surface. These facets were mostly covered with an oxide layer. Dimples of ductile intercrystalline failure (DIF) were located on these facets. A close-up of facets showing ductile intercrystalline failure with dimples (DIF) is provided in Fig. 5. Areas were sometimes also observed in the surface skin where melting of steel occurred. Particles observed in in this area were mostly based on Fe, Mn, S with small amounts of Ti, C and Al.

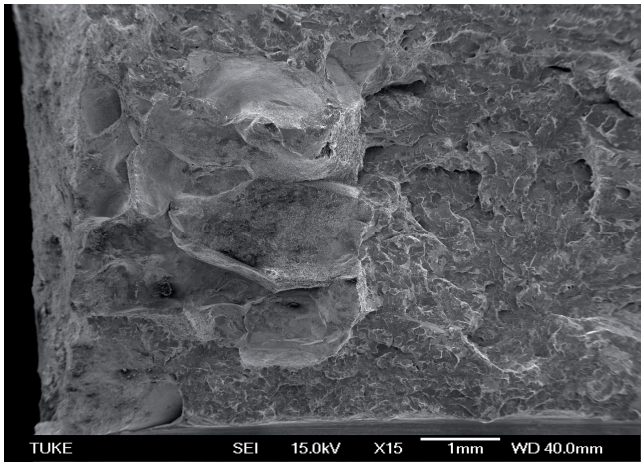

Fig. 4. Coarse intercrystalline facets in the surface skin

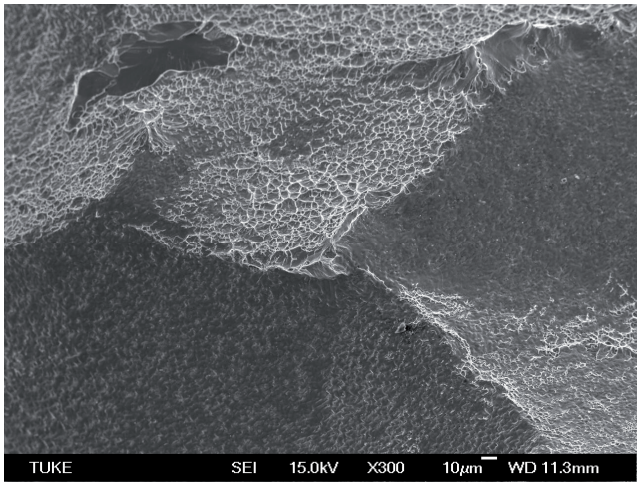

Fig. 5. Detail of DIF with dimples

At the point of the crack below the deep OM on sample A36, the concentration profile of the selected components was determined using WDX analysis. The crack ranged in depth ~5.5 mm below the OM and concentrations of elements were determined at different depths according to the scheme in Figure 2. Figure 6a shows the distribution profiles of elements S, P and N in a plane parallel to the slab surface at a depth of 1 mm below the OM with cracks, where we can see high peaks of sulphur. This area was locally enriched with sulphur, and the max. peak of sulphur concentration reached 1.17%. In this area a high content of nitrogen was also confirmed, which had a max. peak value of 0.64%. Even higher nitrogen content (0.82%) was observed at 4 mm below the OM with cracks. The high content of nitrogen probably indicates the presence of precipitates based on nitrides. In Figure 6b distribution profiles are shown of surface-active elements, namely Sn, Sb and As parallel to the slab surface at a depth of 1 mm below the OM. High content of arsenic was demonstrated, which amounted to max. concentration of 0.26%. Higher content of As was also observed at a depth of 8 mm and even at a depth of 12 mm below the OM, where max. concentrations were in the range 0.13 to 0.20% As. These high concentrations indicate significant segregation of this harmful surface-active element even deeper below the slab surface. The concentrations of the other two elements were lower compared with arsenic. Max. concentration of tin (0.088%) was found at a depth of 12 mm below the OM. Antimony had max. concentration of 0.074% at a depth of 12 mm below the OM.

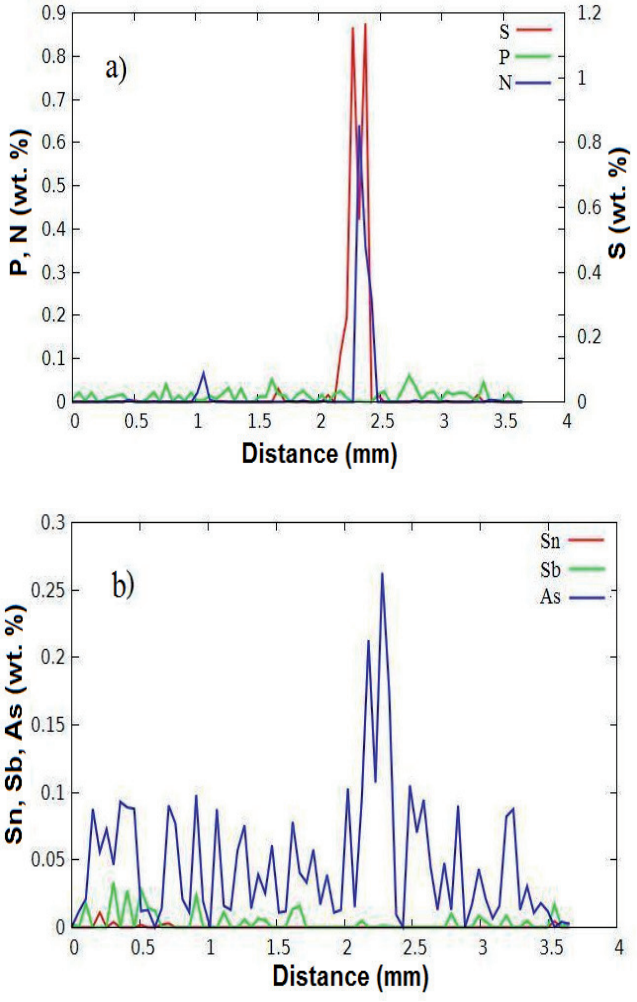

Fig. 6. The spectra of WDX analysis show the varying concentration of components in a plane parallel to the slab surface at a depth of 1 mm below the OM with cracks: (a) S, P, N, (b) Sn, Sb, As

The method of hard X-ray diffraction using the PETRA III positron accelerator at HASYLAB / DESY in Hamburg, produced a diffraction pattern for the sample C12 with cracks which showed that the indexed reflecting planes belonged in the majority phase of α-Fe, while the minor phase was almost unidentifiable. In spite of the fact that the software did not identify the minor phase, the reflections are situated in the detailed diffraction records that are shown in Fig. 7. The record samples C12 identified a total of three secondary phases: Fe_3O_4, TiC and Fe_3C.

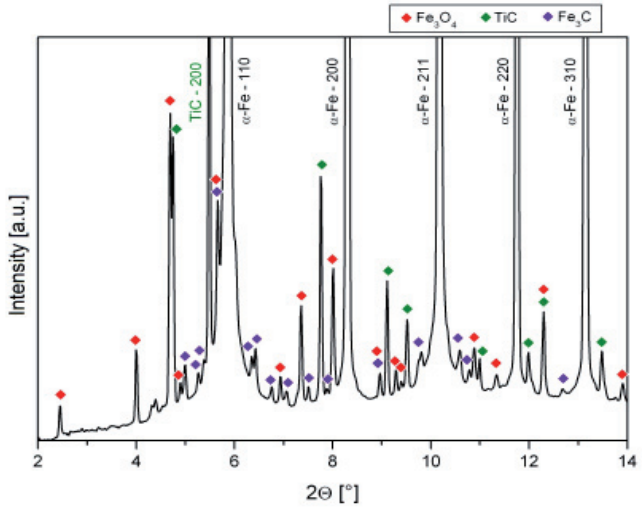

Fig. 7. Detail of diffraction record of the sample C12 with cracks

4. Discussion

The macroscopic analysis shows that on the analyzed surface of the slab no visible surface defects occurred. OM of varying depth were observed on the slab surface. Cut-out test samples revealed the presence of cracks. They were mostly below the OM. After grinding the surface of the slab it was found to be a branched crack (Fig. 3). According to the author of work [1], deep OM increase the susceptibility to the occurrence of transverse cracks by lowering the critical strain, above which cracks form on the surface of continuously-cast semi-finished product. These marks act as a notch for the reduction of the high temperature plasticity of continuously-cast semi-finished products. With increasing depth of OM this notch effect increases, whereby the microstructure is coarser at the bottom of OM due to slower cooling at this site. The bottom of OM is then susceptible to a breach and the formation of cracks, due to stress concentration at the γ-grain boundaries [1,7]. The microstructure was formed of ferritic-pearlitic grains. Tertiary cementite present on the ferritic grain boundaries weakens the cohesion strength of those grain boundaries. Microstructural analysis showed that occasionally the microstructure in the surface skin is characterised by heterogeneity of ferrite grain sizes. Non-equilibrium microstructure of acicular character was observed in the marginal cut-outs. Heterogeneity of microstructure is due to differences in the original austenite grain size, i.e. in some areas in the continuously-cast semi-finished product the surface temperature before phase transformation was different, we suppose because of variation in cooling efficiency, as demonstrated by the works [8,9]. Heterogeneity of the chemical composition of the slab surface skin, e.g. carbon and impurities (P, S, Sn, As) and fracture characteristics in relation to the size of the original austenite grain boundaries have been confirmed, e.g. in works [10,11]. In this work high concentrations of sulphur (1.17%) and arsenic (0.26%) have been shown occasionally, as well as slight increase in Sn (0.088%) and Sb (0.074%). Non-equilibrium microstructure observed in the marginal cut-outs arises due to increased heat dissipation. In works [9,12] it was confirmed that not only the slab cooling rate has an impact on formation of non-equilibrium microstructure, but also the slab pulling rate. The presence of coarse-grained microstructure indicative of coarse-grained original austenitic grain and larger austenite grain also promotes the formation of non-equilibrium microstructure. The slab pulling rate also affects the formation of branched cracks. At lower pulling rates a longer time is available for the progress of segregation processes [13]. The presence of intercrystalline facets on fractures obtained by opening of branched cracks also shows the segregation of harmful impurities and precipitation at the original austenite grain boundaries, which weakens their cohesion strength. Shallow dimples were observed on these coarse intercrystalline facets, i.e. it was a case of intercrystalline ductile failure. The particles in the dimples identified by EDX analysis were mainly based on Fe, Mn, P. Some of these facets were covered with a layer of iron oxide, occasionally also observed on the facets of places where a melt of steel occurred, which may be related to the presence of FeS-type sulphide, whose melting point is 1188°C. At higher concentrations of S eutectic Fe-FeS is formed, whose melting point is relatively low at 988°C [14]. As can be seen in the diffraction record detail in Fig. 7, three phases were then identified in sample C12, namely Fe_3O_4, TiC and Fe_3C. The amounts of Fe_3O_4 and TiC in sample C12 were comparable to the amount of Fe_3C in the analyzed area. According to the authors of work [15] this was also found in connection with particle

precipitation with microalloying elements, resulting in an increased probability of surface crack formation. This is also confirmed in this work, because Fe_3C and also TiC were identified in sample C12 with cracks. Formation of branched cracks in the surface skin of the analyzed slabs made from Ti-Nb microalloyed steel is due to a combination of several factors, namely: lower pulling rate, local segregation of harmful impurities such as S and surface-active elements Sn, Sb, but mostly As. Another factor is the presence of brittle cementite network on the ferritic grain boundaries in combination with TiC.

5. Conclusions

This study of the background of branched crack formation in a continuously-cast Ti-Nb microalloyed steel slab leads to the following conclusions:

1. Visible surface defects do not occur on the analyzed slab surface, and only OM of varying depth were present. Cut-out test samples from the surface skin revealed cracks mostly present below the OM. After grinding the surface of the slab they were found to be a branched crack.
2. Microstructural analysis showed heterogeneity of ferrite grain sizes in the surface skin. Non-equilibrium microstructure was observed in the marginal cut-outs, which formed due to increased heat dissipation.
3. The fracture surfaces from crack opening below the surface skin showed the occurrence of coarse intercrystalline facets, mostly covered with a layer of iron oxide. Dimples on these facets were very shallow, and EDX analysis confirmed the presence of particles at the bottom of these dimples, mainly of MnS type.
4. The results of positron accelerator measurement of sample C12 with cracks showed that in addition to the majority phase of α-Fe, three other phases were identified, namely Fe_3O_4, TiC and Fe_3C, whereby the amount of Fe_3O_4 and TiC was comparable with the amount of Fe_3C in the analyzed area. Particle precipitation with microalloying elements in connection with cementite can lead to higher probability of surface crack formation, as also confirmed in this study.
5. Wavelength-dispersive X-ray analysis showed heterogeneity of chemical composition in the surface skin on the sample with the branched crack. Especially at a depth of 1 mm below the OM with cracks, parallel to the slab surface local accumulation of sulphur was confirmed at a concentration of up to 1.17%, and also nitrogen concentration of 0.64%. The effect of surface-active elements in this area on the formation of cracks was also shown. A high content of arsenic was found with a concentration of up to 0.26%, as well as slight increase in Sn (0.088%) and Sb (0.074%). The increased contents of these elements indicate significant segregation, or otherwise precipitation. Slightly increased contents of N and As were also observed at a depth of 4 mm below the OM. The increased concentration of nitrogen probably indicates the presence of precipitates based on nitrides.
6. Formation of branched cracks in the surface skin of the analyzed slabs made from Ti-Nb microalloyed steel is due to a combination of several factors, namely: lower pulling rate, local segregation of harmful impurities such as S and surface-active elements Sn, Sb, but mostly As. Another factor is the presence of brittle cementite network on ferritic grain boundaries in combination with TiC.

Acknowledgements

This work was supported by project No.1/0387/11 of the Scientific Grant Agency of the Ministry of Education of the Slovak Republic and the Slovak Academy of Sciences and partly due to the project "European Community's Seventh Framework Programme (FP7/2007-2013) under grant agreement n° 312284., DESY proposal n° I-20120037 EC".

References

[1] R. Mišičko, Structure and defects of continuously-cast steel semis, Technical University of Košice, Faculty of Metallurgy, First edition, Emilena, 2007 (in Slovak).

[2] M. Longauerová, Segregation and precipitation at continuous casting, First edition, Technical University of Košice, Faculty of Metallurgy, 2006 (in Slovak).

[3] P. Marek, A. Ševčík, Surface Defects in Low Carbon Steel Slabs, in: M. Longauerová, G. Janák (eds.), The 1st International Conference Physical Metallurgy and Fracture of Materials ´99, Herľany, Slovak Republic, 1999, 261-264.

[4] P. Marek, A. Ševčík, Effect of technological conditions on the surface quality of continuously cast slabs, Oceľové plechy 23/1 (1996) 9-18 (in Slovak).

[5] A. Ševčík, P. Marek, Analysis of the causes of surface defects in continuously cast slabs of steel KOHAL 280, Oceľové plechy 11/1 (1984) 8-11 (in Slovak).

[6] P. Bekeč, M. Longauerová, M. Vojtko, Influence of Casting Rate on TiNb Microalloyed Steel Slab Surface Area Microstructure, Materials Science Forum 782 (2014) 81-86.
[7] Takeuchi, E., Brimacombe, J.K.: Effect of Oscillation-Mark Formation on the Surface Quality of Continuously Cast Steel Slabs, Metallurgical Transactions B 16 (1985) 605-625.
[8] M. Longauerová, Surface microstructural heterogeneity of microalloyed slabs, Conference Contribution of metallography to solving production problems, 14-17.06.2005, Spa Libverda, 28-32 (in Slovak).
[9] M. Longauerová, et al., Effect of Casting Rate on Ti-Nb Microalloyed Steel Slab Surface Zone Microstructure, Acta Metallurgica Slovaca – Conference 1 (2010) 167-172.
[10] M. Longauerová, et al., Distribution of microalloying elements and impurities in surface zone of CC IF steel, Ironmaking and Steelmaking 36/3 (2009) 176-185.
[11] M. Longauerová, et al., Heterogeneity of brittle-fracture properties across width of the slab from IF steel, Proceedings of the Conference Fractography 2006, Stará Lesná, 15-18.10.2006, IMR SAS Košice, Slovak Republic, 220-226 (in Slovak).
[12] P. Bekeč, M. Longauerová, Effect of cooling rate on the microstructure of slabs surface area from Ti-Nb microalloyed steel, Metalurgia Junior 2010, 26-27.05. 2010, Košice, 101-105 (in Slovak).
[13] M. Longauerová, P. Bekeč, M. Vojtko, S. Longauer, P. Marek, Influence of cooling rate on TiNb microalloyed steel slab surface zone fracture morphology, Acta Metallurgica Slovaca – Conference 3 (2013) 30-39.
[14] H. Baker (ed.), ASM Handbook, Alloy Phase Diagrams, Vol. 3, ASM International, 1992.
[15] V. Ludlow, et. al., Understanding the role of microalloy precipitates in the surface cracking of continuously cast slab, Acta Metallurgica Slovaca 13 (2007) 48-57.